

# Simulation protocol of water shut-off treatment for gas storage reservoir in Guantao Field (China)

S. BENALLAOUA<sup>1</sup>, S. ELADJ<sup>1</sup>, A. MIHOUBI<sup>2</sup>, M.Z. DOGHMANE<sup>3</sup> AND M. KELTOUM BENABID<sup>4</sup>

<sup>1</sup> *Laboratory of Earth's Physics, Department of Geophysics, University M'hamed Bougara, Boumerdes, Algeria*

<sup>2</sup> *Department of Seismic Data Processing, SONATRACH, Boumerdes, Algeria*

<sup>3</sup> *Department of Geophysics, University of Science and Technology Houari Boumediene, Bab Ezzouar (Algiers), Algeria*

<sup>4</sup> *Department of Petroleum Engineering, Colorado School of Mines, Golden, CO, U.S.A.*

(Received: 16 November 2022; accepted: 15 February 2023; published online: 13 April 2023)

**ABSTRACT** Nowadays, oil and gas wells can produce excessive amounts of water in many fields. Excessive water production reduces oil and gas productivity by leading to fines and causing sand production and the corrosion of surface facilities. The combination of these unfavourable phenomena results in the early closure of wells as oil and/or gas production becomes unprofitable. In this study, a methodology for simulating water shut-off (WSO) treatments was tested on three synthetic reservoir models in order to conduct sensitivity studies on various parameters affecting the WSO treatment, such as polymer solution type, volume, and injection rate, for the purpose of evaluating different treatment scenarios, defining an optimal treatment design, and forecasting post-treatment well behaviour. Moreover, this protocol explains in detail the different stages of the reservoir simulation methodology for sensitivity analyses and describes the interpretation of WSO treatment results which enable the study of its application feasibility in a real field.

**Key words:** water shut-off (WSO), treatment, sensitivity study, gas storage, reservoir simulation.

## 1. Introduction

Many oil and gas wells around the world may produce excessive amounts of water. This often results in an undesirable loss of productivity, problems with fines, and even equipment corrosion. All of these phenomena can lead to the premature closure of wells since their operating conditions become unprofitable. Many researchers are particularly interested in developing techniques that reduce water inflows. Water shut-off (WSO) treatment is one of the most widely used techniques (Zaitoun *et al.*, 1999; Zaitoun and Pichery, 2001; Sharifpour *et al.*, 2015; Bailón *et al.*, 2020; Putra and Ardiansyah, 2020). This treatment is based on the injection of polymer solutions, containing cross-linker additives, into the producing well: the deeper the solutions penetrate, the higher the permeability of the layers (the main cause of excessive water production), thus reducing the amount of produced water and improving oil or gas production around the well (Al-Muntasheri *et al.*, 2010; Vega *et al.*, 2010; Chaudhary *et al.*, 2016). This technique is integrated into the services offered by some companies (Polymer Well Technology, 2016). The WSO treatment is developed in three stages: laboratory study, simulation study, and field application. This paper focuses on the numerical simulation study of WSO treatments (Luo *et al.*, 2016; Sheshdeh *et al.*, 2016; Alfarge *et al.*, 2017, 2018) and is divided into two parts: the

development of near-wellbore reservoir models and the simulation of WSO treatment.

A WSO treatment protocol was developed using approved efficient simulation software, which included a polymer module with appropriate physical and chemical formulations (Puma Flow, 2016). This methodology was subsequently used to create three different near-wellbore reservoir models and carry out sensitivity studies of the different parameters involved in the WSO treatment. The results obtained firstly allowed to define the best treatment strategy in terms of the type, volume, and concentration of the polymer and of the treatment scenario, and, secondly, to predict long-term reservoir and well behaviour (Sydansk and Seright, 2006). Furthermore, the sensitivity studies have been applied to the different parameters involved in the treatment and defined as follows:

- the maximum pressure reached at the well when injecting a large volume of polymer solution;
- the maximum volume of polymer solution to be injected within the bottomhole pressure (BHP) limit set by the drilling supervisors;
- the effect of the treatment according to the implementation scenario [injection of microgel or gel solution: Chauveteau *et al.* (2004) and Zaitoun *et al.* (2007)].

## 2. Reservoir model construction

### 2.1. Geometry, grid and lithology

In general, a reservoir model should be built around a candidate well over a distance of half length between two wells. The near-wellbore reservoir model constructed for this study is represented by the Cartesian geometry in XYZ, with  $DX = DY = 390$  m, and  $DZ = 38$  m, centred on the well, without dips or fractures (Fig. 1). It is spatially discretised by a corner point grid with a regular mesh. The number of grid cells (meshes) along X and Y is 39, and along Z is 38.

A refined mesh is made in the central grid cell of the well, which is vertically subdivided into 9 cells (3 meshes according to X and Y), therefore the sub-mesh around the well is defined as  $dx =$

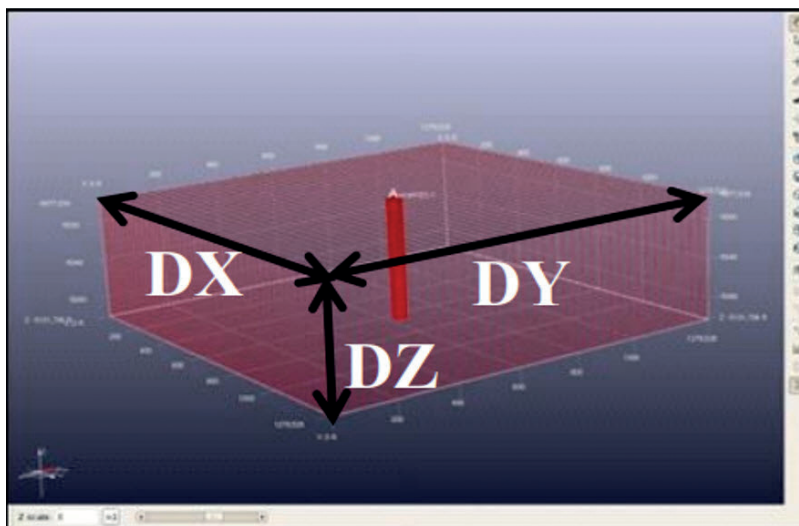


Fig. 1 - The grid and meshes of the designed reservoir models.

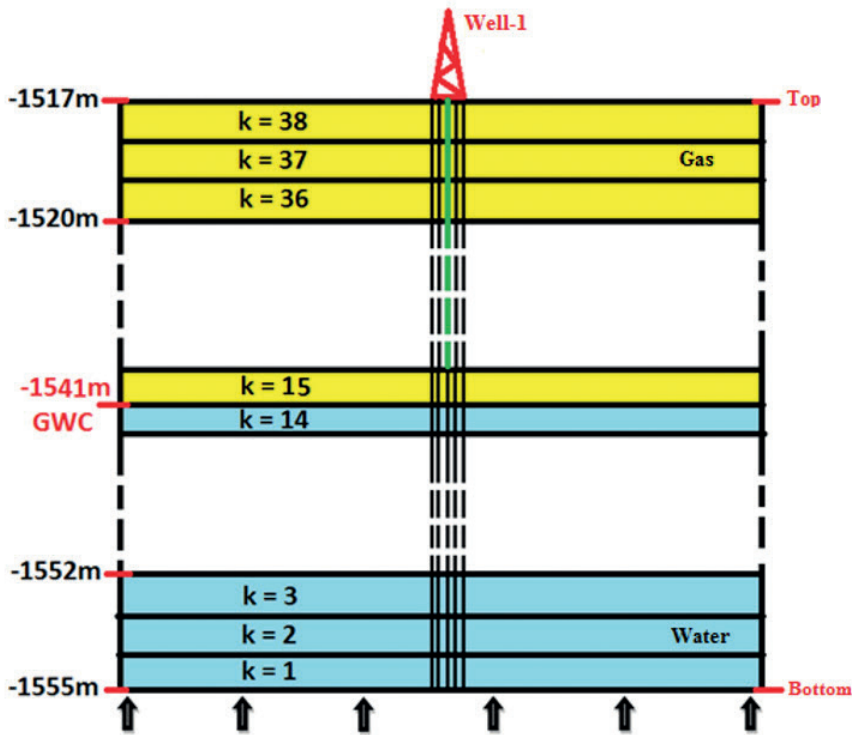


Fig. 2 - A 2D structural model of reservoir with fluids distribution.

$dy = 3.33$  m, and  $dz = 1$  m (Fig. 1). The refined mesh has a volume of  $11.11$  m<sup>3</sup>, while the coarse mesh has a volume of  $100$  m<sup>3</sup>. The top and bottom of the near-wellbore reservoir are at depths of  $1,517$  m, and  $1,555$  m, respectively; this corresponds to a total reservoir thickness of  $38$  m (Fig. 2). The reservoir contains  $38$  isopach layers totalling  $1$  m in thickness, both homogeneous and isotropic, whose facies are determined qualitatively by their porosity and permeability ( $K$ ) values (Thai *et al.*, 2017; Bataee and Irawan, 2018; Wang *et al.*, 2018; Carcione *et al.*, 2020; Doghmane *et al.*, 2022; Eladj *et al.*, 2022a).

## 2.2. The aquifer layer

The studied near-wellbore reservoir models contain a closed aquifer with a steady flow regime of constant water volume. The aquifer considered is represented by a  $12$ -m thick layer under the gas-water contact (GWC). To avoid additional meshes and achieve the desired constant aquifer volume, an analytical aquifer is connected to layer number one ( $k = 1$ ) at the reservoir's bottom, as shown by the arrows in Fig. 2.

## 2.3. Petrophysical properties

Three near-wellbore reservoir models have been created for this study, the only difference between them being the distribution of permeability and porosity (Thai *et al.*, 2017). Rock compressibility is  $5 \times 10^{-10}$  Pa<sup>-1</sup> and vertical transmissibility (a ratio of vertical-to-horizontal permeability) is one-tenth ( $K_v/K_h = 0.1$ ). The gas-water contact is located at a depth of  $1,541$  m (Fig. 2). The aquifer is in a formation with porosity of  $30\%$  and permeability of  $493.5 \times 10^{-15}$

m<sup>2</sup> [500 millidarcy (md): Turner *et al.* (2010); Rad *et al.* (2017)]. The characteristics of the three proposed models are:

- reservoir model 1: the lithology of this multi-layer model is defined in Table 1 (Eladj *et al.*, 2020);
- reservoir model 2: this reservoir model represents a simple case that consists of two types of facies. The first facies corresponds to a high permeability layer ( $H_k$ ) of  $3.45 \times 10^{-12}$  m<sup>2</sup> (3,500 md) and a porosity of 30% with a 12-m thickness of sandstone formation; it is located at the bottom of the reservoir and defined by twelve layers (from layer number 17 to 28). The second facies corresponds to a low permeability layer ( $L_k$ ) of  $394.8 \times 10^{-15}$  m<sup>2</sup> (400 md) and a porosity of 20% with a 10-m thickness of sandstone formation; it is located at the top of the reservoir and defined by ten layers (from layer number 29 to 38) (Da-Xing, 2017). Its lithology is described in Table 1;
- reservoir model 3: this reservoir model represents the opposite case of model 2 in terms of petrophysical properties, thus, an inverse situation of the two types of facies,  $H_k$  and  $L_k$  (Da-Xing, 2017; Doghmane *et al.*, 2018).

Table 1 - Petrophysical properties of the constructed reservoir model.

Layer N°	Depth (m)	Average porosity (fraction)	Average permeability (md)	Lithology
37 to 38	1,517 - 1,519	0.12	10	Clay
35 to 36	1,519 - 1,521	0.22	500	Sandstone ( $L_k$ )
33 to 34	1,521 - 1,523	0.08	10	Clay (restriction zone)
31 to 32	1,523 - 1,525	0.18	100	Sandstone ( $L_k$ )
29 to 30	1,525 - 1,527	0.21	300	Sandstone ( $L_k$ )
27 to 28	1,527 - 1,529	0.08	10	Clay (restriction zone)
25 to 26	1,529 - 1,531	0.25	1000	Sandstone
23 to 24	1,531 - 1,533	0.08	10	Clay (restriction zone)
21 to 22	1,533 - 1,535	0.23	6000	Coarse sandstone ( $H_k$ )
19 to 20	1,535 - 1,537	0.08	10	Clay (restriction zone)
17 to 18	1,537 - 1,539	0.18	100	Sandstone ( $L_k$ )
13 to 16	1,539 - 1,543	0.03	10	Clay (restriction zone)
1 to 12	1,543 - 1,555	0.30	500	Sandstone (aquifer zone)

#### 2.4. Thermodynamic properties of reservoir fluids

The reservoir contains two fluid phases: water and gas. The standard surface conditions of the reservoir's temperature and pressure are  $T_{surf} = 15.5^\circ\text{C}$  and  $P_{surf} = 1.01325 \times 10^5$  Pa, respectively. The most common pressure, volume, and temperature (PVT) data sets for each phase (water and gas) have been taken from the database of the National Institute of Standards and Technologies. For the water phase, the density is  $100.3 \text{ kg/m}^3$ , while the viscosity and volumetric factor ( $\mu_w$  and  $B_w$ , respectively) were introduced as a function of the pressure. For the gas phase, the density is  $8.23 \text{ kg/m}^3$ , while the viscosity and compressibility factor ( $\mu_g$  and  $B_g$ , respectively) were introduced as a function of the pressure (Danesh, 1998).

2.5. Relative permeability and capillary pressure

Figs. 3 and 4 show relative permeability and capillary pressure data that are used and represented for the dry gas sandstone reservoir with a highly wet porous medium (Zhang *et al.*, 2012).

The gas storage well alternates from a gas injector in summer to a gas producer in winter (Wattenbarger, 1970; Bennion *et al.*, 2000; Thompson *et al.*, 2009; De Jong, 2015; Rajabi *et al.*, 2018), and the gas-water fluid system will, therefore, be cyclical in the drainage and imbibition modes. The relative permeability and capillary pressure curves of the two fluids in the drainage and imbibition modes take into account the operating mode of the well.

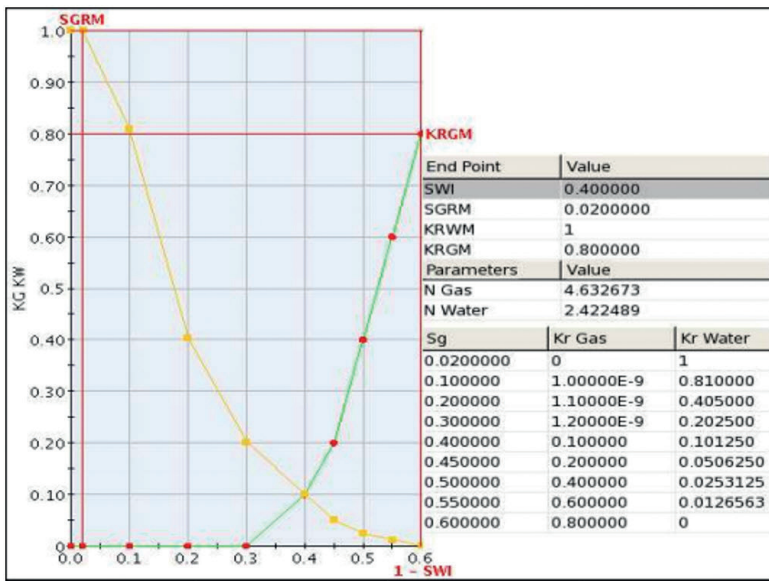


Fig. 3 - Normalised relative permeability data of a water-gas fluid system.

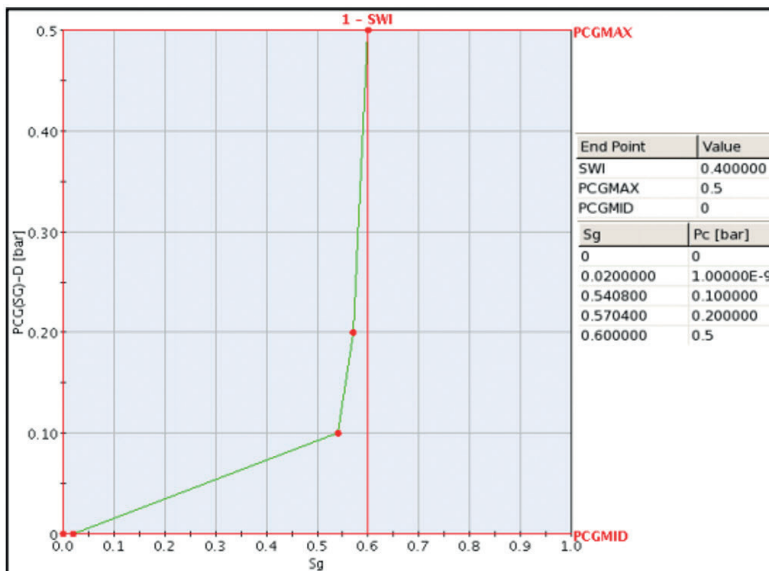


Fig. 4 - Capillary pressure data of a gas-water fluid system.

### 3. Dynamic data and model initialisation

The well has been operated alternately as an injector and as a producer, at a set gas flow rate. The simulation is, therefore, constrained by the gas flow rates shown in Fig. 5. Fig. 5 shows the gas injection and production rates in red and black, respectively. Gas production takes place over a six-month period. There is a one-month period of well shut-in before and after the period of gas injection.

The average gas injection and production rate was 45,000 m<sup>3</sup>/d. The pressure in the well relates to the pressure in the mesh through a productivity index that can be calculated automatically by the designed model, and the imposed pressure limit must be observed. The flow of the two-phase fluids is zero at the lateral borders and at the top of the reservoir; a steady flow of the closed aquifer is at the reservoir bottom. The time zero of the simulation corresponds to the date of 1 October 2005, when the well began to operate in the gas production mode.

The initialisation step is preceded by assuming that the reservoir is at hydrostatic equilibrium. The GWC is at a depth of 1,541 m (between layers 14 and 15). The height of the perforated column begins from the top of the reservoir (-1,517 m) and ends at layer number 17 (-1,539 m). The reservoir reference point for the calculation of pressure and temperature is at a depth of 1,545 m. At this depth, the reservoir temperature is 55°C, and the pressure is 16·10<sup>6</sup> Pa (Fig. 6).

### 4. Simulation of polymer injection

The numerical simulations of water shut-off treatment with polymer have been performed with end user software, a new generation reservoir simulator featuring rigorous physical and

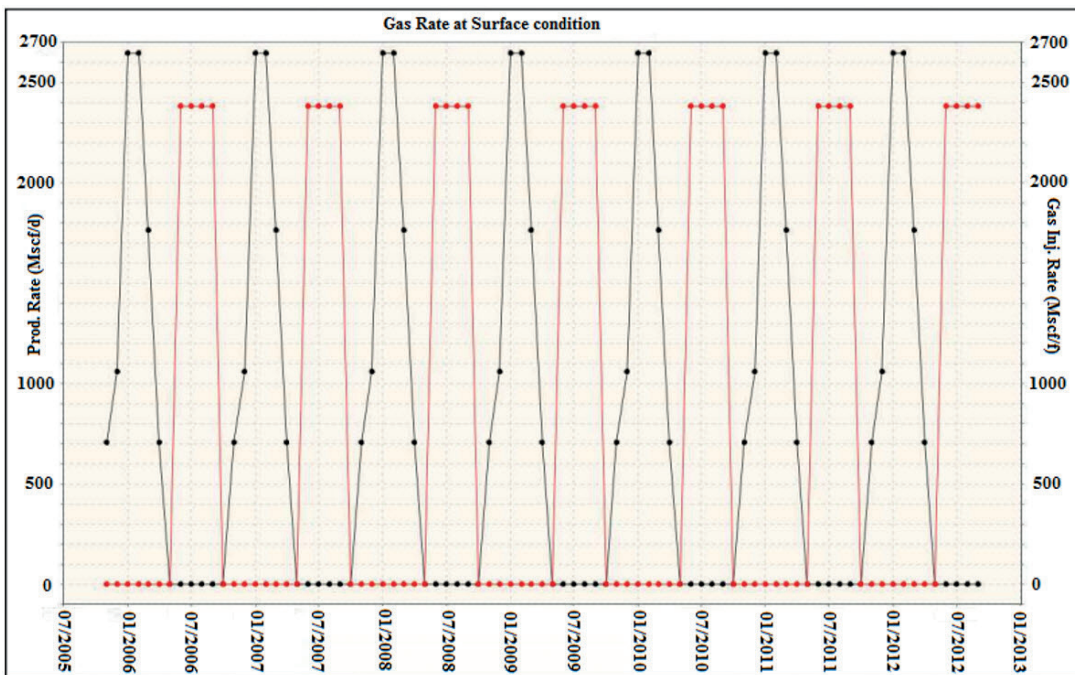


Fig. 5 - Gas injection and production rates of gas storage.

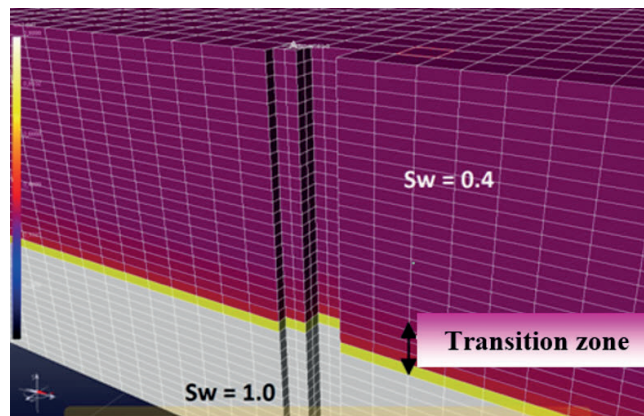


Fig. 6 - Initial state of water saturation on 1 October 2005 storage.

chemical formulations, high performance computing, and a brand-new user-oriented interface. The numerical solvers and numerical schemes have been relentlessly optimised (Eladj *et al.*, 2022b). The software used is compliant with petroleum industry standards (Puma Flow, 2016).

Generally, the polymer solution is injected at the end of the production cycle, when the pressure at the bottom of the well is very low. The software numerical simulation of the polymer injection requires the input of the following parameters obtained from laboratory measurements: molar mass of the polymer ( $1 \times 10^4$  kg/mol), rock density ( $265 \text{ kg/m}^3$ ), maximum polymer adsorption on the rock ( $q_r = 100 \text{ } \mu\text{g/g}$ ), polymer concentration in water (3,000 ppm), permeability reduction table values ( $R_{k_i}$ ) according to the polymer concentration for the different rock types (Liang and Seright, 2001; Ogunberu and Asghari, 2005).

Three types of rocks have been defined for these reservoirs:

- rock type 1: absolute permeability greater than  $987 \times 10^{-15} \text{ m}^2$  (1,000 md);
- rock type 2: absolute permeability between  $98.7 \times 10^{-15} \text{ m}^2$  and  $987 \times 10^{-15} \text{ m}^2$  (100 md and 1,000 md);
- rock type 3: absolute permeability less than  $98.7 \times 10^{-15} \text{ m}^2$  (100 md).

Polymer adsorption on the rock wall of the porous medium causes the reduction in permeability, which in turn causes the reduction in mobility at a zero polymer concentration in the water phase (Ogunberu and Asghari, 2005; Sun *et al.*, 2009). The microgel/gel solution was injected on 1 May 2012 (end of the gas production cycle). The gas injection rate was constrained by the pressure limit and the polymer solution injectivity (Gussenov *et al.*, 2014; Luo *et al.*, 2016). Next, a gas injection cycle was carried out in order to enable resaturating the area surrounding the well (Rad *et al.*, 2017; Bataee and Irawan, 2018).

## 5. Sensitivity tests on WSO treatments

The purpose of the sensitivity tests is to assess the effectiveness of the treatment with various parameters and define the optimal treatment design (Vega *et al.*, 2010; Alfarge *et al.*, 2017, 2018).

The sensitivity tests can determine: 1) sensitivity of injected gel solution volumes, 2) sensitivity of the permeability reduction value, 3) sensitivity of injected microgel solution volumes, 4) sensitivity of the injectivity rate of gel or microgel solution.

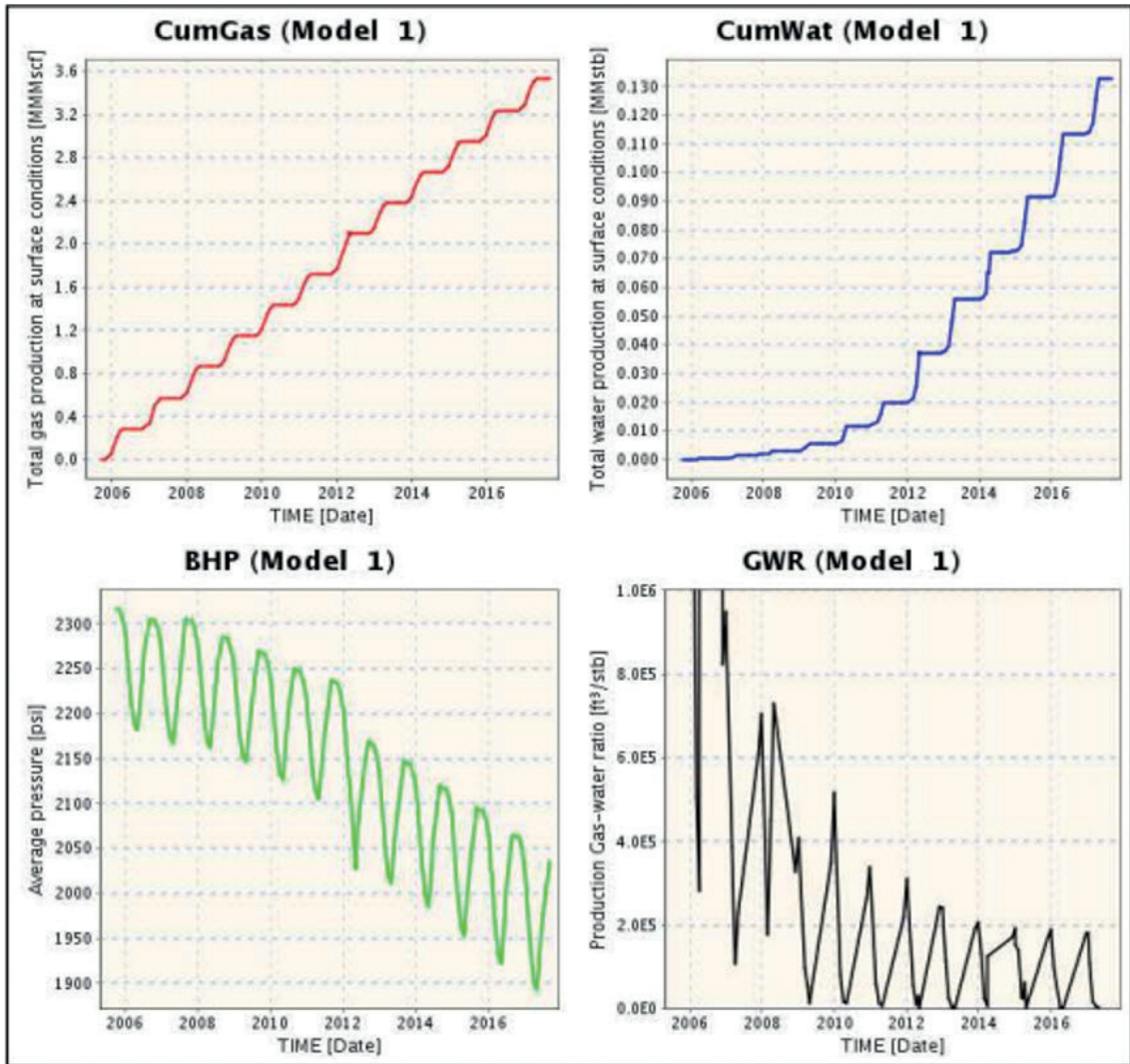


Fig. 7 - Simulation results without treatment.

The simulation results without treatment, shown in Fig. 7, were used as a reference for the evaluation of the other tests. For all scenarios, the WSO preventive treatment is carried out on the same date (1 May 2012). Within five years of treatment, the reservoir simulations were evaluated for a total of twelve years.

### 5.1. Relative permeability and capillary pressure

In this part, several scenarios for injecting a gel solution slug have been evaluated on reservoir model 1. According to Figs. 7 and 8, the cumulative amount of water produced without treatment in October 2017 was around 21,000 m<sup>3</sup>.

- Test 1:  $V_g = 50 \text{ m}^3$ ,  $R_k = 50$ , and  $K > 987 \times 10^{-15} \text{ m}^2$  (1,000 md). A treatment was first carried out by injecting 50 m<sup>3</sup> of gel solution, with a reduction permeability value ( $R_k$ ) equal to 50, assigned to the zone of high permeability ( $H_k$ ) ( $K > 1,000 \text{ m}^3$ ), and relating only to two



layers (N° 21 and N° 22). According to the results in Fig. 8, the cumulative amount of water produced after using this treatment was around 7,400 m<sup>3</sup>. This treatment reduces the cumulative production water by approximately 65%.

- Test 2:  $V_g = 25 \text{ m}^3$ ,  $R_k = 50$ , and  $K > 987 \times 10^{-15} \text{ m}^2$  (1,000 md). A treatment was carried out by injecting 25 m<sup>3</sup> of gel, with an  $R_k$  value equal to 50, assigned to the zone of high permeability ( $H_k$ ) ( $K > 1,000 \text{ md}$ ). According to the results in Fig. 8, this treatment reduces the cumulative production of water by approximately 60%. Comparing the reduction of cumulative water production between the two tests, test 2 is almost as effective at reducing water inflows as test 1 with half the gel volume. This gel volume value will be set and used for the remainder of the tests.

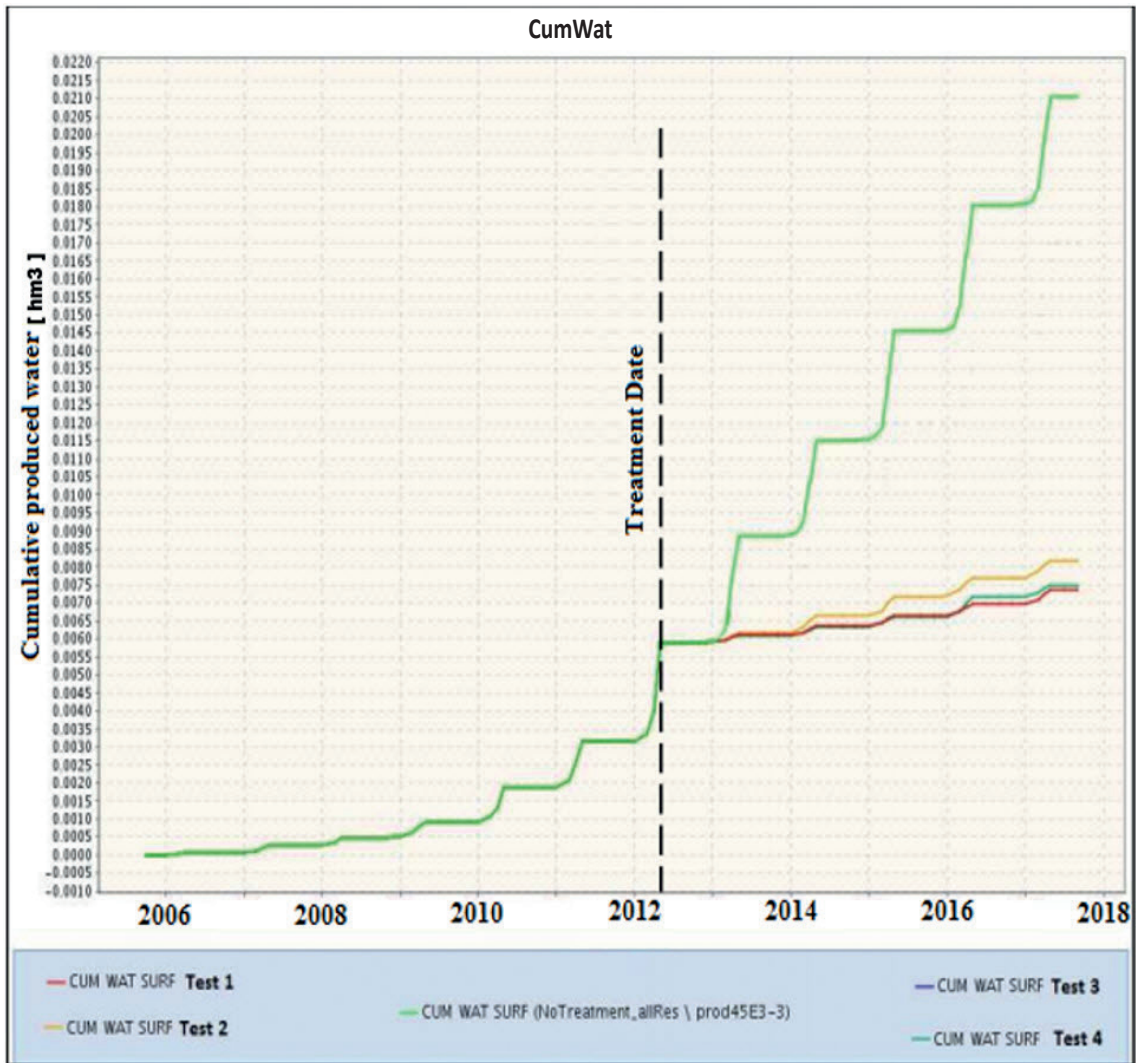


Fig. 8 - Cumulative amount of produced water for different gel treatment tests.

## 5.2. Sensitivity tests on the permeability reduction value

- Test 3:  $V_g = 25 \text{ m}^3$ ,  $R_k = 90$ , and  $K > 987 \times 10^{-15} \text{ m}^2$  (1,000 md). In test 3, test 2 was repeated with the only modification consisting in a different  $R_k$  value, increased to a value of 90. According to the results given in Fig. 8, this treatment reduces the cumulative amount of produced water by approximately 65%, which is identical to test 1 and a little more than test 2.
- Test 4:  $V_g = 25 \text{ m}^3$ ,  $R_k = 90$ , and  $K > 493.5 \times 10^{-15} \text{ m}^2$  (500 md). In test 4, test 3 was repeated with the only modification of the allocation of the permeability reduction by rock type to  $K > 500 \text{ md}$ . Layers N° 21, 22, 25, and 26 of reservoir model 1 were affected by the permeability reduction. The simulation results of test 4 are identical to those of test 3. The reduction in the total amount of produced water is the same as that obtained in Fig. 8. This result confirms the hypothesis that the influx of water comes mainly from the two most permeable layers that play the role of channels fed by the aquifer's ascent.

It is also noted from the results of the four tests that the optimal gel solution is the one used in test 3 ( $V = 25 \text{ m}^3$ ,  $R_k = 90$ , and  $K > 1,000 \text{ md}$ ). With its optimised parameters, this gel slug has reduced the total amount of produced water by approximately 65% while using only a volume of  $25 \text{ m}^3$ . However, it has had a minor impact on the BHP (reduction of  $5 \times 10^5 \text{ Pa}$  with the same amount of produced gas), as illustrated in Fig. 9. Therefore, the use of gel slugs is very effective in preventing the inflow of water from the highly permeable layers that are above an aquifer (Turner *et al.*, 2010).

Table 2 summarises the results of the various gel treatment tests in terms of reduction of cumulative water production compared to the volume of water produced without treatment (about  $21,000 \text{ m}^3$ ).

Table 2 - Reduction of water production in the different gel treatment tests.

Test number	Water reduction (%)
01 ( $V = 50 \text{ m}^3$ , $R_k = 50$ with $K > 1,000 \text{ md}$ )	65
02 ( $V = 25 \text{ m}^3$ , $R_k = 50$ with $K > 1,000 \text{ md}$ )	60
03 ( $V = 25 \text{ m}^3$ , $R_k = 90$ with $K > 1,000 \text{ md}$ )	65
04 ( $V = 25 \text{ m}^3$ , $R_k = 90$ with $K > 500 \text{ md}$ )	64

## 5.3. Sensitivity analysis with different injected microgel volumes

The WSO treatment sensitivity study with the use of microgel solution alone (without gel slug) has been analysed by varying its volume. A reduction in water production was expected with the increase in the injected microgel volume ( $V_{mg}$ ). The objective of these tests is to compare the effectiveness of an injection of a large volume of microgel against a limited volume of gel (Vega *et al.*, 2010).

### 5.3.1. Sensitivity tests on the microgel volume for reservoir model 1

The volume series of injected microgel in reservoir model 1 were:  $25 \text{ m}^3$ ,  $100 \text{ m}^3$ , and  $1,000 \text{ m}^3$ . Fig. 10 represents the cumulative amount of produced water after treatment for different microgel volumes.



Fig. 9 - Effect of gel injection treatment on bottomhole pressure for reservoir model 1.

As expected, the results of Fig. 10 show that the more the volume of microgel injected increases, the greater the reduction in the quantity of produced water. As the reduction in water production corresponding to the treatment with a microgel volume of 1,000 m<sup>3</sup> (blue curve) is similar to that obtained with a volume ten times less (red curve), it is not necessary to test an additional microgel volume greater than 1,000 m<sup>3</sup>. Table 3 summarises the results of WSO treatment tests with microgel for reservoir model 1 in terms of produced water reduction rate with their corresponding injected microgel volumes.

Table 3 - Water reduction rate of treatment tests with different injected microgel volumes in reservoir model 1.

Microgel volume (m <sup>3</sup> )	25	100	1,000
Water reduction (%)	17	20	21

Among the different results obtained with the sensitivity tests on the microgel volume, the optimal scenario of a WSO treatment with microgel is the one corresponding to the injection of 100 m<sup>3</sup> of microgel into the reservoir.

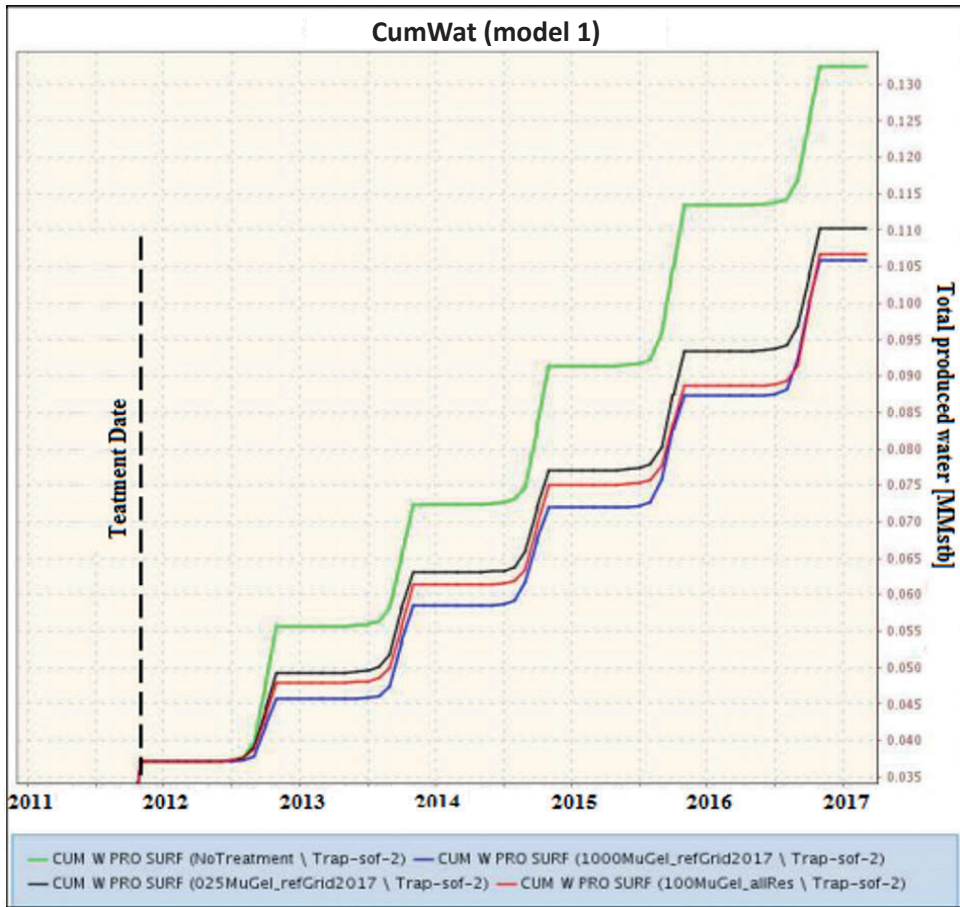


Fig. 10 - Cumulative amount of produced water after treatment for different injected microgel volumes in reservoir model 1.

Reservoir model 1 is comparable to a reservoir model used in a similar work by Zaitoun *et al.* (2007). Although the two similar studies used different WSO treatment parameters and simulators, they had the same order of magnitude and trend of simulation results (stair-step trend for the cumulative water production results and oscillatory trend for the bottomhole pressure results). See Figs. 8 and 9 of this paper and compare them with Figs. 8 and 10 of Zaitoun *et al.* (2007). As they are validated by an acceptable history match before and after treatment with actual field data, the simulation results of the similar work have a low degree of uncertainty. Consequently, the results illustrated in this paper are valid with low uncertainty.

### 5.3.2. Sensitivity tests of microgel volume for reservoir model 2

For reservoir model 2, the series of injected microgel volumes were: 100 m<sup>3</sup>, 1,000 m<sup>3</sup>, 3,000 m<sup>3</sup>, 5,000 m<sup>3</sup>, 7,000 m<sup>3</sup>, and 9,000 m<sup>3</sup>. According to the results in Fig. 11, the optimal scenario of treatment for this model is the one corresponding to the injection of 7,000 m<sup>3</sup> of microgel. As the reduction in water production corresponding to a treatment with a microgel volume of 9,000 m<sup>3</sup> (black curve) is not as big as that obtained with a volume of 7,000 m<sup>3</sup> (blue curve), it is not necessary to test an additional microgel volume greater than 9,000 m<sup>3</sup>.

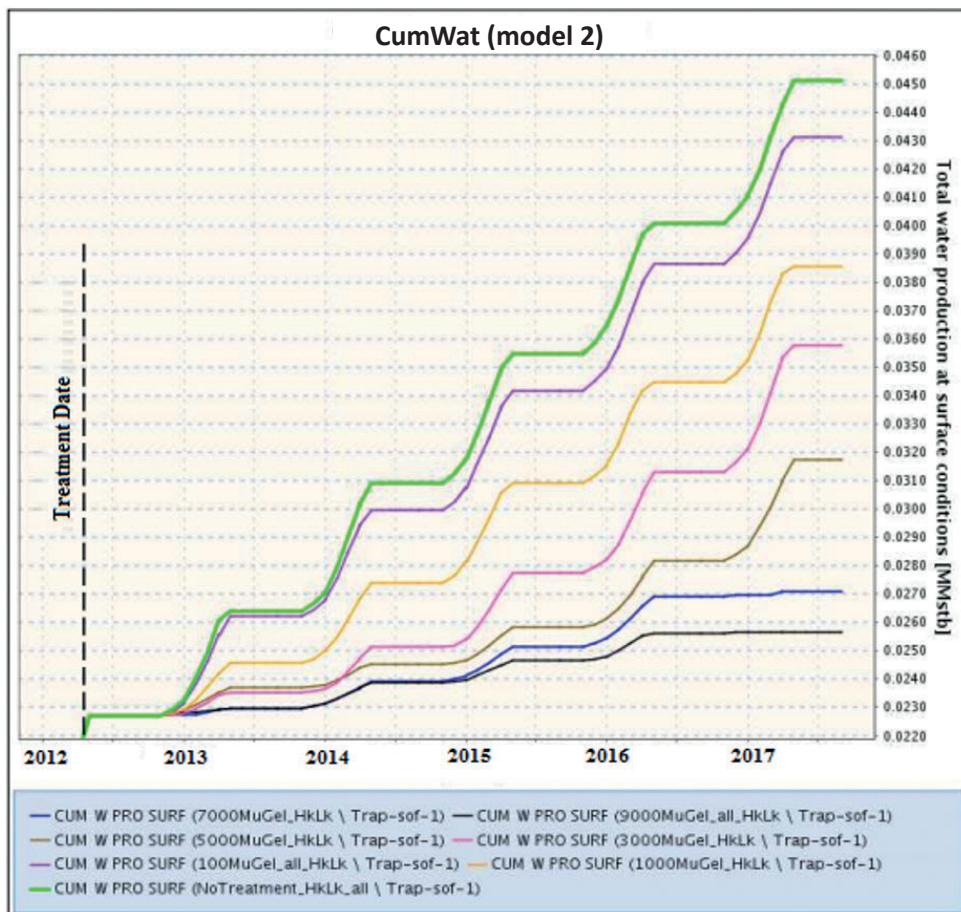


Fig. 11 - Cumulative amount of produced water after treatment for different injected microgel volumes in reservoir model 2.

However, it was not easy to deal with a large volume of microgel because it could generate a high cost for the production that had been stopped for a long time. The BHP value remains acceptable even with a large volume of microgel injected into the reservoir (Fig. 12).

Table 4 summarises the results of WSO treatment tests by microgel for reservoir model 2 in terms of produced water reduction rate, with their corresponding injected microgel volume.

Table 4 - Water reduction rate of treatment tests with different injected microgel volumes in reservoir model 2.

Microgel volume (m <sup>3</sup> )	100	1,000	3,000	5,000	7,000	9,000
Water reduction (%)	5	15	20	29	40	44

### 5.3.3. Sensitivity tests of microgel volume for reservoir model 3

For reservoir model 3, the series of injected microgel volumes were: 25 m<sup>3</sup>, 100 m<sup>3</sup>, 1,000 m<sup>3</sup>, and 3,000 m<sup>3</sup>. According to Fig. 13, the optimal scenario of treatment for this model is the one corresponding to the injection microgel volume of 1,000 m<sup>3</sup> (blue curve). As the reduction

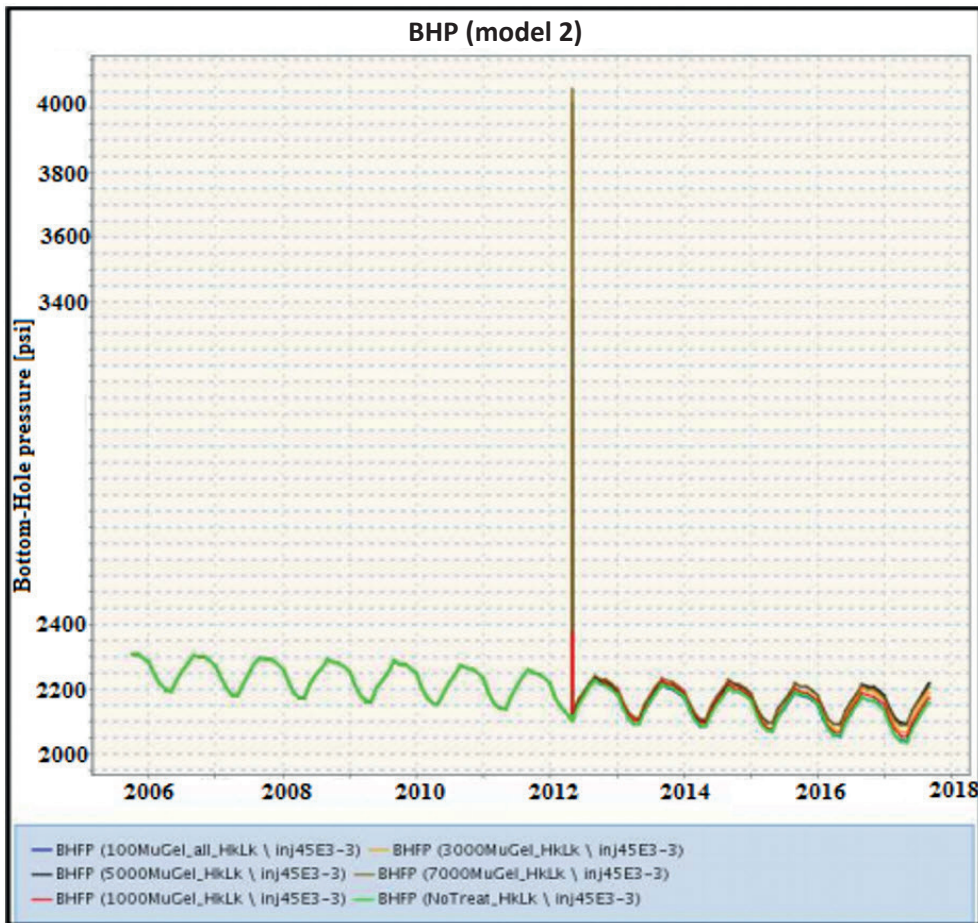


Fig. 12 - Effect of microgel injection treatment on bottomhole pressure for reservoir model 2.

in water production corresponding to the treatment with a microgel volume of 3,000 m<sup>3</sup> (purple curve) is similar to that obtained with a volume three times less (blue curve), it is not necessary to test an additional microgel volume greater than 3,000 m<sup>3</sup>. Table 5 summarises the results of WSO treatment tests by microgel for reservoir model 3 in terms of produced water reduction rate with their corresponding injected microgel volume.

Table 5 - Water reduction rate of treatment tests with different injected microgel volumes in reservoir model 3.

Microgel volume (m <sup>3</sup> )	25	100	1,000	3,000
Water reduction (%)	9	23	28	27

There is a clear correlation between the water reduction rate and the injected microgel volume for all reservoir models.

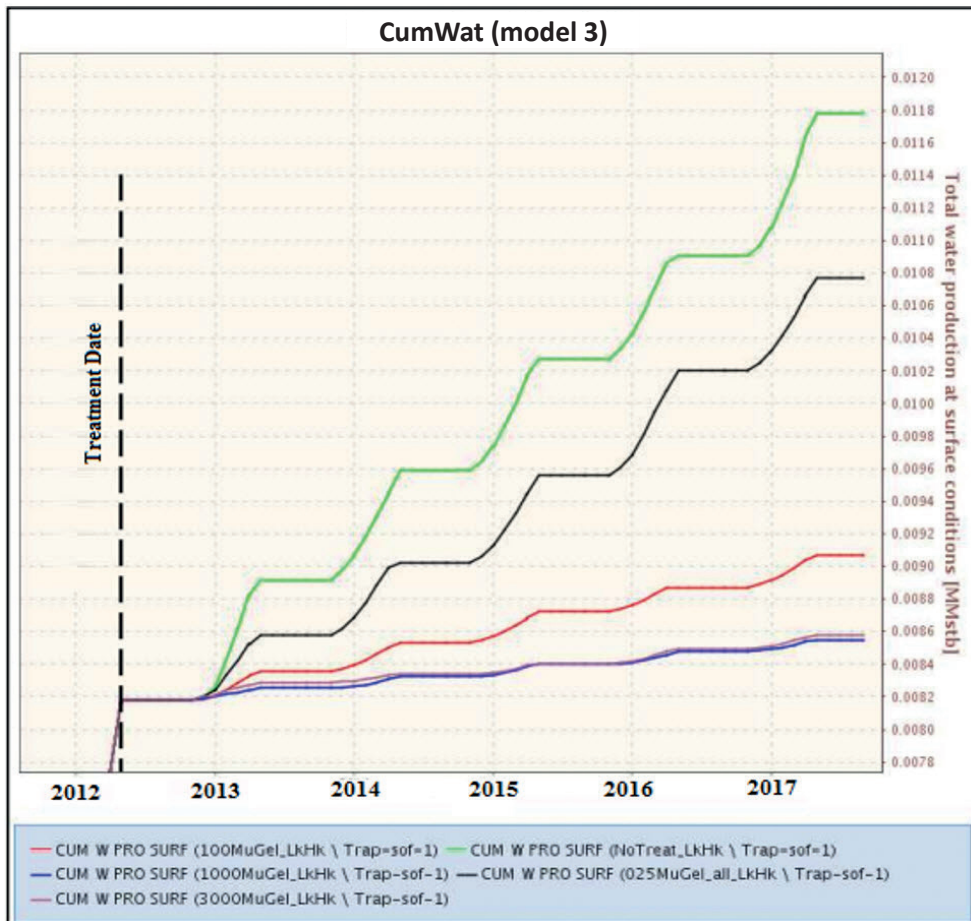


Fig. 13 - Cumulative amount of produced water after treatment for different injected microgel volumes in reservoir model 3.

#### 5.3.4. Sensitivity analysis to the injectivity rate of the product (gel or microgel)

The purpose of the product injectivity test was to assess the pressure reached at the bottom of the well when the product (gel or microgel) was injected (Luo *et al.*, 2016). For each simulation carried out, the value of the BHP was calculated, knowing that a pressure difference less than  $3 \times 10^6$  Pa (440 Psi) is generally acceptable in practice, whereas any greater value could be problematic.

## 6. Performance comparison

Conclusions can be drawn from a comparative study in terms of effectiveness between the best gel-based treatment and the best microgel-based treatment applied to each of the studied reservoir models. The best gel-based treatment used for this comparison corresponds to the one chosen in the first sensitivity study (Test 3) carried out on reservoir model 1. This treatment was applied to the other two reservoir models 2 and 3. Figs. 14, 15, and 16 represent the cumulative water production results obtained from the gel and microgel optimal treatments applied to

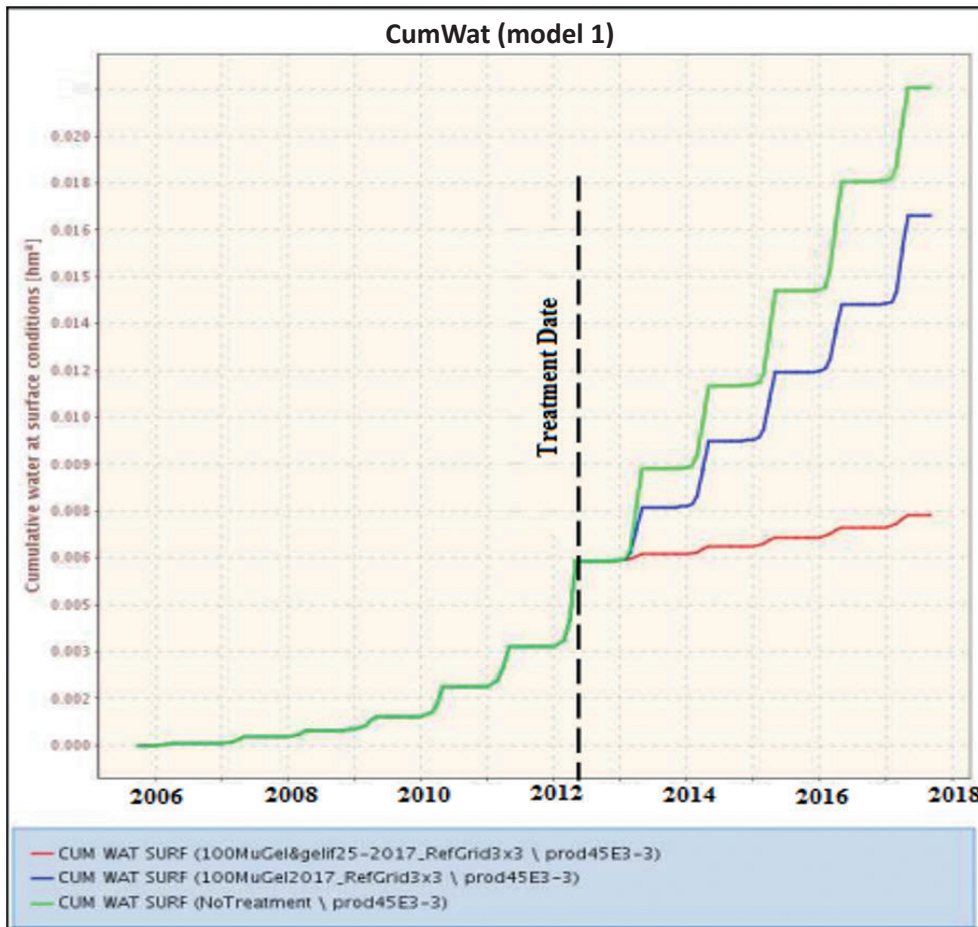


Fig. 14 - Cumulative water production of gel and microgel optimal treatments for reservoir model 1.

studied reservoir models 1, 2, and 3, respectively. Table 6 summarises the water reduction rate of the optimal treatment based on gel and microgel for each reservoir model.

Table 6 - Comparison of water production rate between gel and microgel optimal treatments for all reservoir models.

		WSO optimal treatment based on microgel	WSO optimal treatment based on gel
Water reduction rate (%)	Reservoir model 1	20	65
	Reservoir model 2	40	47
	Reservoir model 3	27	28

It is noted that the treatment based on a limited gel volume produces superior, better, or similar performance in terms of water reduction rate than the one based on a large microgel volume for the studied reservoir models (Alfarge *et al.*, 2018). Based on these results, the performance of WSO treatments is sensitive to the petrophysical model (the main difference



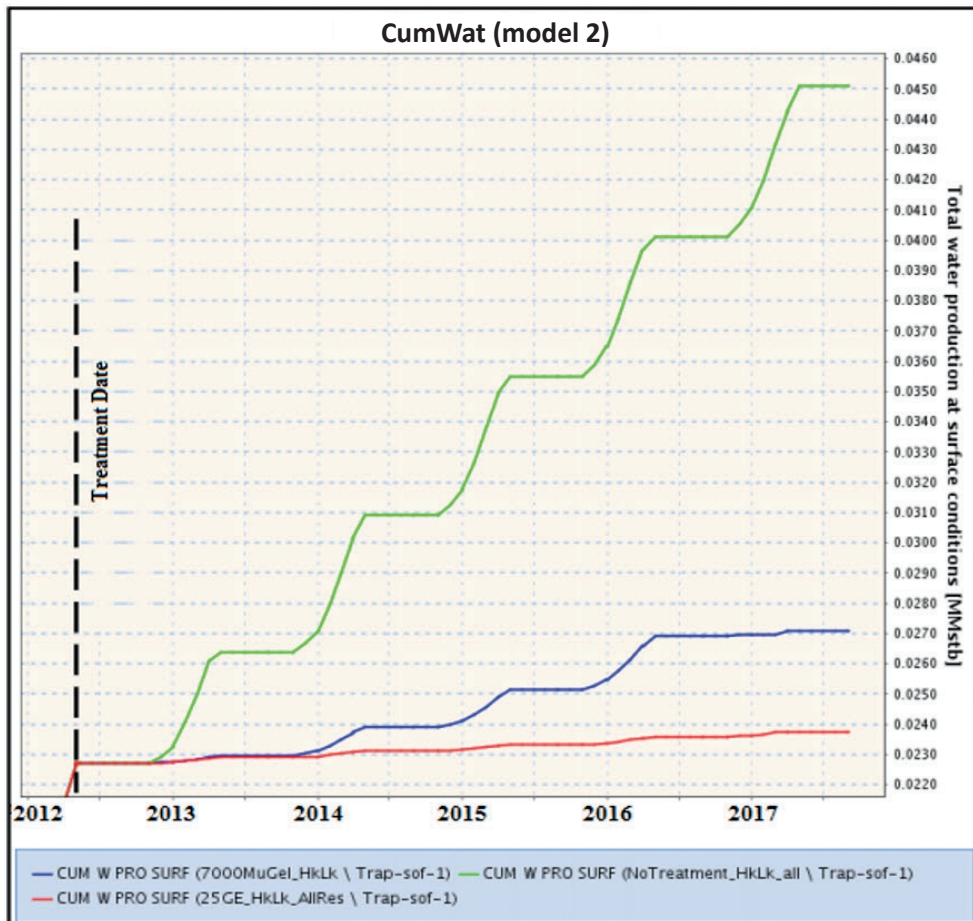


Fig. 15 - Cumulative water production of gel and microgel optimal treatments for reservoir model 2.

between the three studied reservoir models) and could be excellent by using a small gel slug for a reservoir model with very high permeability streaks (reservoir model 1).

## 7. Conclusions

Sensitivity studies of water shut-off treatment provided by a simulation protocol proved that the effectiveness of the treatment, based on a limited volume of gel for different petrophysical configurations of gas storage reservoirs, has little impact on a well's bottomhole pressure. Nonetheless, the treatment using a large volume of microgel can achieve similar results to the gel-based treatment, but generates much higher reservoir pressure and significant costs. The simulation protocol developed in this study has been successfully tested on several reservoir models using petroleum industry-approved reservoir simulation software with a practical graphical interface instead of a restrictive and impractical simulation by keyword files. Therefore, the proposed simulation can be a powerful and essential tool to assess the feasibility and effectiveness of the WSO treatment before its application in the field.

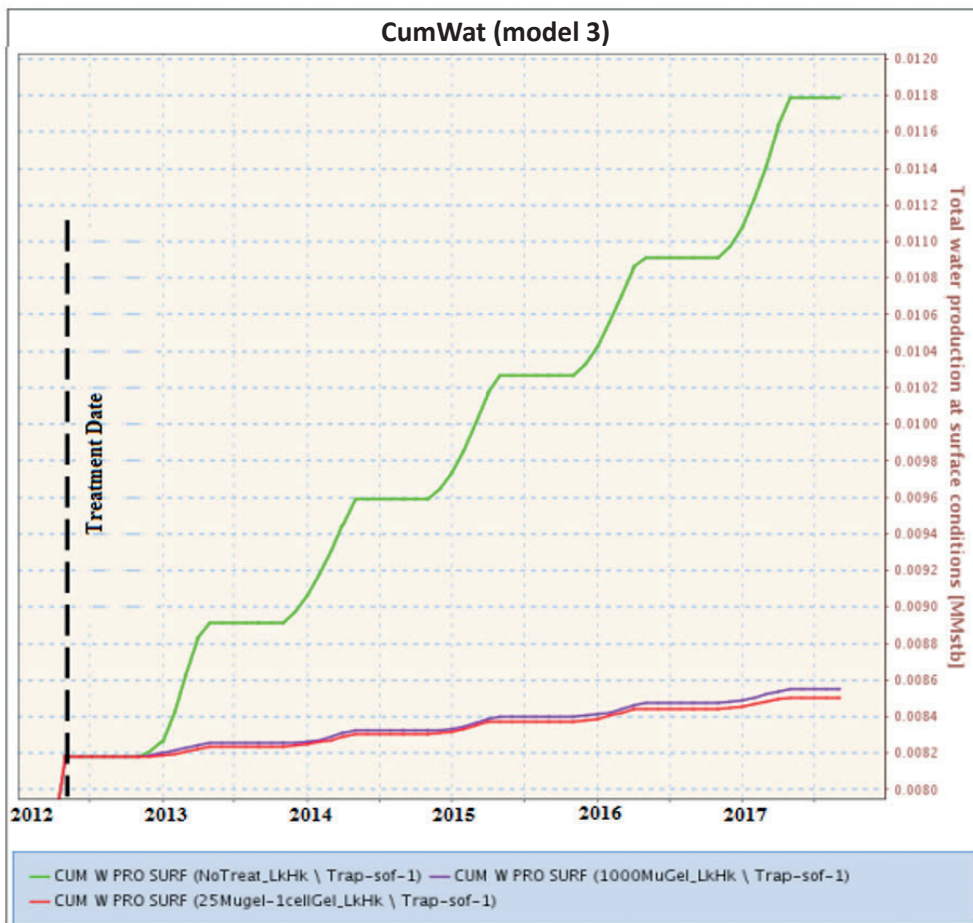


Fig. 16 - Cumulative water production of gel and microgel optimal treatments for reservoir model 3.

## REFERENCES

- Al-Muntasheri G.A., Sierra L., Garzon F., Lynn J.D. and Izquierdo G.; 2010: *Water shut-off with polymer gels in a high temperature horizontal gas well: a success story*. In: Proc. SPE/DOE Symposium on Improved Oil Recovery, Tulsa, OK, USA, SPE-129848-MS, doi: 10.2118/129848-MS.
- Alfarge D.K., Wei M. and Bai B.; 2017: *Numerical simulation study of factors affecting relative permeability modification for water-shutoff treatments*. Fuel, 207, 226-239, doi: 10.1016/j.fuel.2017.06.041.
- Alfarge D., Wei M., Bai B. and Almansour A.; 2018: *Numerical simulation study to understand the performance of RPM gels in water-shutoff treatments*. J. Pet. Sci. Eng., 171, 818-834, doi: 10.1016/j.petrol.2018.07.082.
- Bailón L.R., Orellana N.H., Villegas S., Martinez E., Román S., Espín J., Gaibor A. and Tamayo T.; 2020: *The water shut off technique extends the productive life cycle of the cretaceous U sandstone: the Iro field case in Ecuador*. In: Proc. SPE Latin American and Caribbean Petroleum Engineering Conference, Virtual, Society of Petroleum Engineers, SPE-199070-MS, doi: 10.2118/199070-MS.
- Bataee M. and Irawan S.; 2018: *Porosity and permeability alteration around wellbore during injection process*. Int. J. Geomech., 18, 04017145, doi: 10.1061/(ASCE)GM.1943-5622.0001051.
- Bennion D.B., Thomas F.B., Ma T. and Imer D.; 2000: *Detailed protocol for the screening and selection of gas storage reservoirs*. In: Proc. SPE/CERI Gas Technology Symposium, Calgary, AB, Canada, SPE-59738-MS, doi: 10.2118/59738-MS.
- Carcione J.M., Gei D., Picotti S., Misnan M.S., Rashidi M.R.A., Bakar Z.A.A., Harith Z.Z.T., Bahri N.H.S. and Hashim N.; 2020: *Porosity and permeability of the overburden from wireline logs: a case study from offshore Malaysia*. Geomech. Geophys. Geo-Energy Geo-Resour., 6, 1-12, doi: 10.1007/s40948-020-00172-y.

- Chaudhary P., Kumar S. and Reddy S.; 2016: *Polymer and its role in EOR and water shut-off process*. J. Basic Appl. Eng. Res., 3, 717-720.
- Chauveteau G., Tabary R., Blin N., Renard M., Rousseau D. and Faber R.; 2004: *Disproportionate permeability reduction by soft preformed microgels*. In: Proc. SPE/DOE Symposium on Improved Oil Recovery, Tulsa, Ok, USA, SPE-89390-MS, doi: 10.2118/89390-MS.
- Da-Xing W.; 2017: *A study on the rock physics model of gas reservoir in tight sandstone*. Chin. J. Geophys., 60, 64-83, doi: 10.1002/cjg2.30028.
- Danesh A.; 1998: *PVT and phase behaviour of petroleum reservoir fluids, 1st ed*. Elsevier, Amsterdam, The Netherlands, 398 pp.
- De Jong C.; 2015: *Gas storage valuation and optimization*. J. Nat. Gas Sci. Eng., 24, 365-378, doi: 10.1016/j.jngse.2015.03.029.
- Doghmane M.Z., Belahcene B. and Kidouche M.; 2018: *Application of improved artificial neural network algorithm in hydrocarbons' reservoir evaluation*. In: Hatti M. (ed), Renewable energy for smart and sustainable cities: artificial intelligence in renewable energetic systems, ICAIRES 2018, Lecture Notes in Networks and Systems, Springer, Cham, Switzerland, vol. 62, pp. 129-138, doi: 10.1007/978-3-030-04789-4\_14.
- Doghmane M.Z., Ouadfeul S.A., Benaissa Z. and Eladj S.; 2022: *Classification of Ordovician tight reservoir facies in Algeria by using Neuro-Fuzzy algorithm*. In: Hatti M. (ed) Artificial intelligence and heuristics for smart energy efficiency in smart cities: case study: Tipasa, Algeria, ICAIRES 2021, Lecture Notes in Networks and Systems, Springer, Cham, Switzerland, vol. 361, pp. 889-895, doi: 10.1007/978-3-030-92038-8\_91.
- Eladj S., Lounissi T.K., Doghmane M.Z. and Djeddi M.; 2020: *Lithological characterization by simultaneous seismic inversion in Algerian South Eastern Field*. Eng. Technol. Appl. Sci. Res., 10, 5251-5258.
- Eladj S., Doghmane M.Z. and Belahcene B.; 2022a: *Design of new model for water saturation based on neural network for low-resistivity phenomenon (Algeria)*. In: Proc. 2nd Springer Conference of the Arabian Journal of Geosciences, Advances in Geophysics, Tectonics and Petroleum Geosciences, CAJG-2, Advances in Science, Technology and Innovation, Springer, Cham, Switzerland, pp. 325-328, doi: 10.1007/978-3-030-73026-0\_75.
- Eladj S., Doghmane M.Z., Aliouane L. and Ouadfeul S.A.; 2022b: *Porosity model construction based on ANN and seismic inversion: a case study of Saharan Field (Algeria)*. In: Proc. 2nd Springer Conference of the Arabian Journal of Geosciences, Advances in Geophysics, Tectonics and Petroleum Geosciences, CAJG-2, Advances in Science, Technology and Innovation, Springer, Cham, Switzerland, pp. 241-243, doi: 10.1007/978-3-030-73026-0\_55.
- Gussenov I., Ibragimov R.S., Kudaibergenov S., Abilkhairov D.T. and Kudaibergenov D.N.; 2014: *Application of polymer gellan for injectivity profile leveling*. In: Proc. SPE Annual Caspian Technical Conference and Exhibition, Astana, Kazakhstan, SPE-172299-MS, doi: 10.2118/172299-MS.
- Liang J. and Seright R.S.; 2001: *Wall-effect/gel-droplet model of disproportionate permeability reduction*. SPE J., 6, 268-272, doi: 10.2118/74137-PA.
- Luo H.S., Delshad M., Li Z.T. and Shahmoradi A.; 2016: *Numerical simulation of the impact of polymer rheology on polymer injectivity using a multilevel local grid refinement method*. Pet. Sci., 13, 110-125, doi: 10.1007/s12182-015-0066-1.
- Ogunberu A.L. and Asghari K.; 2005: *Water permeability reduction under flow-induced polymer adsorption*. J. Can. Pet. Technol., 44, 56-61, doi: 10.2118/05-11-06.
- Polymer Well Technology; 2016: Poweltec, Rueil Malmaison, France, <www.poweltec.com/>.
- Puma Flow; 2016: Reservoir simulation software, Beicip-Franlab S.A., Paris, France, <www.beicip.com/reservoir-simulation>.
- Putra D. and Ardiansyah M.; 2020: *Optimizing water shut off (WSO) by utilizing cross-linker additive system in the nearby wellbore treatment in sandstone environment*. Mater. Today: Proc., 39, 1020-1024, doi: 10.1016/j.matpr.2020.04.757.
- Rad H.S., Rajabi M. and Masoudian M.S.; 2017: *A numerical study of gas injection and caprock leakage from Yort-e-Shah aquifer in Iran*. Eng. Technol. Appl. Sci. Res., 7, 1843-1849.
- Rajabi M., Rad H.S. and Masoudian M.S.; 2018: *A numerical model for caprock analysis for subsurface gas storage applications*. Eng. Technol. Appl. Sci. Res., 8, 2438-2446.
- Sharifpour E., Riazi M. and Ayatollahi S.; 2015: *Smart technique in water shutoff treatment for a layered reservoir through an engineered injection/production scheme*. Ind. Eng. Chem. Res., 54, 11236-11246, doi: 10.1021/acs.iecr.5b02191.

- Sheshdeh M.J., Awemo K.N. and Yadav A.; 2016: *Simulation case study of water shut-off with RPM gels in an oil field in northern Germany*. In: Proc. SPE Bergen One Day Seminar, Grieghallen, Bergen, Norway, SPE-180062-MS, doi: 10.2118/180062-MS.
- Sun Y., Liu C., Su W., Zhou Y. and Zhou L.; 2009: *Principles of methane adsorption and natural gas storage*. Adsorp., 15, 133-137, doi: 10.1007/s10450-009-9157-x.
- Sydansk R.D. and Seright R.S.; 2006: *When and where relative permeability modification water-shutoff treatments can be successfully applied*. In: Proc. SPE/DOE Symposium on Improved Oil Recovery, Tulsa, OK, USA, SPE-99371-MS, doi: 10.2118/99371-MS.
- Thai B., Van Tran X., Do K.Q., Hoang Q.T. and Nguyen T.M.; 2017: *Applying the evaluation results of porosity-permeability distribution characteristics based on hydraulic flow units (HFU) to improve the reliability in building a 3D geological model, GD field, Cuu Long Basin*. J. Pet. Explor. Prod. Technol., 7, 687-697, doi: 10.1007/s13202-017-0334-2.
- Thompson M., Davison M. and Rasmussen H.; 2009: *Natural gas storage valuation and optimization: a real options application*. Nav. Res. Logist., 56, 226-238, doi: 10.1002/nav.20327.
- Turner B.O., Nwaozo J. and Funston B.C.; 2010: *Quantitative evaluation of aquifer diversion to surrounding wells after multiple large polymer gel water shutoff treatments*. In: Proc. SPE Production and Operations Conference and Exhibition, Tunis, Tunisia, SPE-132978-MS, doi: 10.2118/132978-MS.
- Vega I.N., Morris W., Robles J.L., Peacock H. and Marin A.; 2010: *Water shut-off polymer systems: design and efficiency evaluation based on experimental studies*. In: Proc. SPE Symposium on Improved Oil Recovery, Tulsa, OK, USA, SPE-10.2118/129940-MS, doi: 10.2118/129940-MS.
- Wang Y., Sun S. and Gong L.; 2018: *Study on numerical methods for gas flow simulation using double-porosity double-permeability model*. In: Proc. 18th International Conference, Computational Science, ICCS 2018, Lecture Notes in Computer Science, Springer, Cham, Switzerland, 10862, pp. 129-138, doi: 10.1007/978-3-319-93713-7\_10.
- Wattenbarger R.A.; 1970: *Maximizing seasonal withdrawals from gas storage reservoirs*. J. Pet. Technol., 22, 994-998, doi: 10.2118/2406-PA.
- Zaitoun A. and Pichery T.; 2001: *A successful polymer treatment for water coning abatement in gas storage reservoir*. In: Proc. SPE Annual Technical Conference and Exhibition, New Orleans, LA, USA, SPE-71525-MS, doi: 10.2118/71525-MS.
- Zaitoun A., Kohler N., Bossie-Codreanu D. and Denys K.; 1999: *Water shutoff by relative permeability modifiers: lessons from several field applications*. In: Proc. SPE Annual Technical Conference and Exhibition, Houston, TX, USA, SPE-56740-MS, doi: 10.2118/56740-MS.
- Zaitoun A., Tabary R., Rousseau D., Pichery T., Nouyoux S., Mallo P. and Braun O.; 2007: *Using microgels to shut off water in a gas storage well*. In: Proc. International Symposium on Oilfield Chemistry, Houston, TX, USA, SPE-106042-MS, doi: 10.2118/106042-MS.
- Zhang Y., Li H. and Yang D.; 2012: *Simultaneous estimation of relative permeability and capillary pressure using ensemble-based history matching techniques*. Transp. Porous Media, 94, 259-276, doi: 10.1007/s11242-012-0003-3.

*Corresponding author:* Said Eladj  
Department of Geophysics, Faculty of Hydrocarbons and Chemistry, University M'hamed Bougara  
Avenue Independence, Boumerdes 35000, Algeria  
Phone: +213 24 795 267; email: .eladj@univ-boumerdes.dz